AGU PUBLICATIONS

JGR

Journal of Geophysical Research: Space Physics

RESEARCH ARTICLE

10.1002/2014JA019982

Key Points:

- Widely used diffusive equilibrium models of the plasmasphere are evaluated
- Qualitative and quantitative comparisons to an empirical model and observations
- Mathematical form/physical assumptions of the model are incompatible with observations

Correspondence to:
P. Ozhogin,
ozhogin@gmail.com

Citation:
Ozhogin, P., P. Song, J. Tu, and B. W. Reinisch (2014), Evaluating the diffusive equilibrium models: Comparison with the IMAGE RPI field-aligned electron density measurements, *J. Geophys. Res. Space Physics*, *119*, 4400–4411, doi:10.1002/2014JA019982.

Received 13 MAR 2014
Accepted 20 MAY 2014
Accepted article online 23 MAY 2014
Published online 5 JUN 2014

Evaluating the diffusive equilibrium models: Comparison with the IMAGE RPI field-aligned electron density measurements

P. Ozhogin[1,2], P. Song[1,2], J. Tu[1,2], and B. W. Reinisch[1,3]

[1]Center for Atmospheric Research, University of Massachusetts Lowell, Lowell, Massachusetts, USA, [2]Physics Department, University of Massachusetts Lowell, Lowell, Massachusetts, USA, [3]Lowell Digisonde International, LLC, Lowell, Massachusetts, USA

Abstract The diffusive equilibrium models that are widely used by the space physics community to describe the plasma densities in the plasmasphere are evaluated with field-aligned electron density measurements from the radio plasma imager (RPI) instrument onboard the IMAGE satellite. The original mathematical form of the diffusive equilibrium model was based on the hydrostatic equilibrium along the magnetic field line with the centrifugal force and the field-aligned electrostatic force as well as a large number of simplifying approximations. Six free parameters in the mathematical form have been conventionally determined from observations. We evaluate four sets of the parameters that have been reported in the literature. The evaluation is made according to the equatorial radial distance dependence, latitudinal dependence at a given radial distance, and the combined radial and latitudinal dependences. We find that the mathematical form given in the diffusive equilibrium model is intrinsically incompatible with the measurements unless another large number of free parameters are artificially introduced, which essentially changes the nature of a theoretical model to an empirical model.

1. Introduction

The Earth's plasmasphere, a region in space dominated with higher density and lower temperature plasma of ionospheric origin, plays significant roles in space weather [e.g., *Lemaire and Gringauz*, 1998]. One of the roles is that the plasmasphere is the medium in which plasma waves propagate and interact with energetic particles. Because the plasma density distribution determines the propagation velocities of very low frequency, extremely low frequency, and ultralow frequency waves and the resonance conditions for the wave-particle interactions, it is important to study, understand, and accurately model the plasmasphere in order to determine the characteristics and propagation of plasma waves which strongly influence the ring current and radiation belts dynamics. The plasmasphere itself is dense (density 10^2–10^4 cm^{-3}) and consists of cold (temperature ~1 eV) plasma. It does not have a well-defined lower boundary with the ionosphere, although conventionally it is considered to be above the 1000 km altitude. The outer boundary, the plasmapause, can be either pronounced and sharp, or gradual, or even have complex structures [e.g., *Nagai et al*., 1985; *Horwitz et al*., 1990; *Sandel et al*., 2003; *Carpenter and Lemaire*, 2004; *Tu et al*., 2007], although conventionally the location of the plasmapause is known to be controlled by the balance between the corotation and the magnetospheric convection.

Since the discovery of the plasmasphere [*Storey*, 1953], there have been needs for a model that would adequately describe the distribution of the cold plasma. However, in the early 1960s only extremely limited satellite and rocket sounding measurements were available, and the computational abilities were rather restricted. Thus, empirical and numerical models were understandably coarse. The solution came after the development of a theoretical model that is referred to as the diffusive equilibrium (DE) model. It has been and still is widely used by the space physics community. For example, it is utilized in a number of ray tracing codes [e.g., *Kimura*, 1966; *Inan and Bell*, 1977; *Starks et al*., 2008; *Bortnik et al*., 2011; *Sonwalkar et al*., 2011], and it is applied to derive equatorial densities from ground measurements of whistler waves [e.g., *Angerami and Carpenter*, 1966; *Helliwell et al*., 1973; *Park*, 1973; *Inan et al*., 1977; *Kimura*, 1966]. A similar approach is also used in studying space plasmas [e.g., *Vranjes and Tanaka*, 2005]. Even though significant progress in the development of empirical and numerical models has been made, the diffusive equilibrium model has often been used as a protocol, but it has not been carefully tested and verified. This is because the DE model describes the plasma density distribution along a magnetic field line, yet such measurements were not available until recently.

The diffusive equilibrium model was described in great detail in an earlier work by *Angerami and Thomas* [1964]. We like to point out that although it was named "diffusive equilibrium," it was based on the equations of hydrostatic, in contrast to convective, equilibrium radial from the Earth with an electrostatic force that acts on ions and electrons, and no diffusion process is involved. The diffusiveness actually refers to varying mixing ratios of heavy ions with height. In addition to the hydroequilibrium assumption, the most important assumption is that the ratios of the electron temperature to that of every heavy ion species are independent on height. Derived with seven key assumptions, the model calculates the electron and ion densities along a magnetic field line in the plasmasphere based on multiple input parameters: electron density and ion composition (H^+, He^+, O^+) at a base level (along that magnetic field line) in the ionosphere and the temperature (electron or ion) in the plasmasphere. The resulting density is given as a function of a temperature-modified geopotential height (z), although it is common knowledge that the temperature distribution critically depends on the density distribution for a hydrostatic equilibrium. In other words, assuming a temperature distribution specifies in principle the density distribution, and no new information is gained.

Generally, the temperatures of ions and electrons are different from each other, and both vary with altitude and latitude. Most DE model applications make, however, the following two simplifying assumptions: (1) electron and ion temperatures are equal to each other and (2) the plasmasphere is isothermal, i.e., its temperature is the same everywhere in the plasmasphere. The result is that the geopotential height (z) does not depend on temperature, thus making an analytical solution for z possible.

Another assumption that is used in practical applications is the absence of the centrifugal force. This makes the geopotential height (z) independent of latitude. The resulting expression for the geopotential height (which we will refer to as z' in order to avoid the confusion with the original expression of *Angerami and Thomas* [1964]) becomes equivalent to the one used by *Bauer* [1962] and *Kimura* [1966]:

$$z'(R) = \frac{R_B}{R}(R - R_B), \tag{1}$$

where R is the geocentric distance to the point of interest and R_B is the geocentric distance to the base of the diffusive equilibrium model.

Thus, the resulting diffusive equilibrium equation takes the following compact form [e.g., *Kimura*, 1966; *Inan and Bell*, 1977]:

$$N_e(R) = N_B N_{\mathrm{DE}}(R), \tag{2}$$

where N_B is the reference electron density at the base of the diffusive equilibrium model and N_{DE} is the diffusive equilibrium term:

$$N_{\mathrm{DE}}(R) = \sqrt{\sum_{i=1}^{3} \eta_i \exp(-z'(R)/H_i)}, \tag{3}$$

where η_i are the relative concentrations of ionic species at R_B and $i = 1, 2, 3$ correspond to H^+, He^+, O^+, respectively. The scale height H_i for ion species i is defined as

$$H_i = \frac{k_B T_{\mathrm{DE}}}{m_i g(R_B)}, \tag{4}$$

where k_B is the Boltzmann constant, T_{DE} is the temperature at the base of the diffusive equilibrium model (and, thus, everywhere for an isothermal plasmasphere), m_i is the corresponding ion species mass, and $g(R_B) = 9.81$ $(R_E/R_B)^2$ is the value of gravitational acceleration, in m s^{-2}, at the base of a diffusive equilibrium model.

With so many assumptions some of which may or may not be valid, there is an additional critical issue that was discussed by *Angerami and Thomas* [1964]. It is the fact that N_B is a constant for a particular field line but can be different for different field lines. *Carpenter and Smith* [1964] also recognized this issue and pointed out the fact that the freedom of this model is so large that it can fit any given measurements if they were made along a satellite orbit which crosses different field lines. Therefore, the model cannot be validated by in situ observations that are made from different field lines, unless at the same time N_B is also measured along each

Table 1. Values of Input Parameters, All From the Original References: the Altitude of the Base of the Diffusive Equilibrium Model, Temperature, Electron Density, and Ion Composition (H^+, He^+, and O^+) at the Base Level

				DE-B
Parameter	DE-1	DE-2	DE-S2	DE-B*
R_B (km)	500	1,000	1180	1000
T_{DE} (K)	1,000	1,000	1700	1600
N_B (cm^{-3})	34,600	10,000	7645	3100
H^+ (%)	0.2	15.2	40	8
He^+ (%)	1.9	82.3	30	2
O^+ (%)	97.9	2.5	30	90

field line crossed by the satellite. One then may question the validity to use it for ray tracing, for example, if the ray is not simply along a single field line with a known density at the base.

Until recently, all measurements of electron and ion densities in the plasmasphere have been made in situ. Since satellites generally do not move along a single field line, it was impossible to experimentally verify with such in situ measurements the correctness of the diffusive equilibrium description of the field-aligned distribution of plasma. With the data from the radio plasma imager (RPI) instrument onboard the IMAGE satellite [*Burch*, 2000], we are now able to determine the electron density profile along a single magnetic field line [*Reinisch et al.*, 2001, 2009] almost instantaneously (within 1–2 min, depending on the sounding program used). Making use of this capability, we evaluated the diffusive equilibrium model by comparing it with measurements of the field-aligned electron density profiles obtained from the RPI active sounding experiments from June 2000 to July 2005.

In the following section we briefly describe the RPI electron profile database, the empirical model derived from it, and the differences between four diffusive equilibrium models used in this evaluation. In sections 3 we evaluate the models by studying the resulting equatorial and off-equatorial density distributions. We present the quantitative results of the evaluation and of a case study that investigates the causes of the differences.

2. Database and Evaluation Methods

The field-aligned density measurements from the IMAGE RPI instrument are described in detail in a number of publications [e.g., *Reinisch et al.*, 2001; *Song et al.*, 2004; *Huang et al.*, 2004]. In brief, the RPI was a low-power radar (<10 W pulse power) that operated in the frequency range from 3 kHz to 3 MHz. The active sounding data are presented in the form of "plasmagrams," which display the amplitude of the returned signal as a function of virtual range and frequency. Often, discrete echo traces with enhanced signal strength are observed on a plasmagram. One type of these traces is formed by the signals that propagate along the magnetic field line through satellite [*Reinisch et al.*, 2001; *Fung and Green*, 2005]. By using an inversion algorithm [*Huang et al.*, 2004], one can derive the electron densities along the individual magnetic field line from one plasmagram containing almost instantaneous measurements. A database consisting of more than 700 density profiles was compiled and used to derive an empirical model of the electron densities in the plasmasphere [*Ozhogin et al.*, 2012]. The electron density (in cm^{-3}) can be expressed as a function of L shell (L) and magnetic latitude (λ):

$$N(L,\lambda) = Neq(L)\cdot \cos^{-0.75}\left(\frac{\pi}{2}\cdot\frac{\lambda}{\lambda_{\mathrm{INV}}}\right), \quad Neq(L) = 10^{(4.4693-0.4903\cdot L)}, \tag{5}$$

where λ_{INV} is the magnetic invariant latitude.

The RPI also performed dynamic spectral measurements in passive mode. An upper hybrid resonance band on these dynamic spectrograms [e.g., *Benson et al.*, 2004] can be used to determine the plasmapause location with a high level of certainty and accuracy (within 0.1–0.2 L in the cases of sharp plasmapause boundary) [*Tu et al.*, 2007]. All of the over 700 electron density profiles used in this study have been manually confirmed to be within the plasmasphere, earthward of the plasmapause boundary. These profiles covered all magnetic local times (MLTs) rather uniformly. Since no strongly pronounced MLT dependence has been found at the time, this makes the comparison of the models fair, since the DE model is MLT independent as well.

The diffusive equilibrium models that we are evaluating in this study can be driven with a broad range of input parameters. As it is impossible to cover all variations of the parameters used, we analyze the output results of a representative set of input values. The four diffusive equilibrium models (see Table 1 for the values of the input parameters) that have been chosen in this study are the following: DE-1 and DE-2 from *Kimura* [1966], DE-S2 from *Sonwalkar et al.* [2011], and DE-B* from *Bortnik et al.* [2011]. First three models use the same functional form of the original DE model and the same set of parameters. The differences are the reference values at the model base. The fourth model, DE-B* [*Bortnik et al*., 2011], may be considered significantly different from a diffusive equilibrium model because the substantial modification has removed many characteristics of the diffusive equilibrium. It multiplies the electron densities of the diffusive equilibrium model, referred to in the following as DE-B, by a combination of six additional parameters, which brings the total number of fitting parameters to 12. This dramatically changes the density distribution. Additionally, *Sonwalkar et al*. [2011] presented a model, referred to as DE-S1 that uses a different set of parameters (column 1 of Table 1 in their paper). However, the outcome of DE-S1 is extremely close to that of DE-S2 in the range of L shells of interest (1.5–4.5).

It can be seen from Table 1 that even though some of the models (DE-2, DE-S2, and DE-B) use almost the same base level around 1000 km altitude, the reference electron densities can differ by a factor of 3, temperatures by a factor of 1.7, and ion compositions by factors from 2.6 to 36. Even though there is a possibility that the plasma densities, composition, and temperature vary significantly at ~1000 km, such wide spread in parameters makes it difficult for a user to select a certain parameter set, and furthermore, to justify any particular choice, unless there has been a satellite or a rocket measurement that could provide such data.

Ray tracing programs usually require the knowledge of the plasma densities everywhere, not just in the plasmasphere; thus, they employ additional terms in equation (2), namely, at the lower ionosphere (N_{LI}) and at the plasmapause (N_{PL}). Since no RPI electron density profile in our database goes below 600 km altitude, we can safely ignore the lower ionosphere term [*Bortnik et al*., 2011; *Sonwalkar et al*., 2011] during the evaluation given below. Furthermore, since all electron density profiles used in this study are manually confirmed to be inside of the plasmasphere, we can ignore the plasmapause term as well.

It is worth clarifying that in the approach of *Kimura* [1966], the electron density is assumed to be a product of the radially varying density and a colatitudinal factor ($N_e = N_r \times N_\theta$). *Kimura* [1966] considered the situation when the latitudinal effect is modeled by a sinusoidal or linear dependence on colatitude. These dependences were chosen to simulate ionospheric horizontal irregularities of particular shapes in order to reproduce a very specific effect—so-called subprotonospheric whistlers [*Carpenter et al*., 1964]. If the linear dependence is chosen, the densities decrease with increasing latitude. In contrast, the sinusoidal dependence results in a plasmasphere with very sharp density gradients with a period of 10° (see Figure 12 of *Kimura* [1966]), since per *Kimura* [1966]: "The half period of the sine function was chosen to be approximately equal to the latitudinal interval between the entrance and exit of the one-hop ray path." These functional forms may be suitable only for a narrow latitudinal region, but when calculating the ray tracing in the whole plasmasphere [*Kimura*, 1966], the colatitude factor N_θ is assumed constant and equals one, which leads to N_e to be equivalently equal to N_B in equation (2). Therefore, in order to make a fair evaluation in the plasmasphere region, we assume the constant colatitude function when discussing the DE-1 and DE-2 models.

As different authors have employed slightly different approaches to describing the diffusive equilibrium models they used, it is worth resolving the following issue: the scale height H_i at a particular base level (R_B), described by equation (4), can be calculated for H^+ and then just divided by 4 or 16 to get the scale heights for He^+ and O^+, respectively, assuming that different species are in thermal equilibrium. For a 1000 km altitude, if we use the following constants: $k_B = 1.3807 \times 10^{-23}$ (m^2 kg s^{-2} K^{-1}), $m_{H+} = 1.6726 \times 10^{-27}$ (kg), $g = 7.33$ (m s^{-2}), we obtain $H_{H+} = 1.1262{*}T_{DE}$ (km), where T_{DE} is in Kelvins. However, *Sonwalkar et al*. [2011] use 1.1506 as the multiplier, and *Inan and Bell* [1977] list 1.506, which might have been a typographical error. Even though the difference between factors 1.1262 and 1.1506 is not very large (within 2%), the resulting difference may be significant in a quantitative comparison, as the DE equation involves an exponential function. We have used 1.1506 when programming the code for implementing DE-S1 and DE-S2 and 1.1262 when working with DE-1, DE-2, and DE-B. We have successfully reproduced the plasma densities or plasma frequencies for the examples shown in the original references, so we are confident having faithfully represented those models.

3. Model Evaluation

3.1. Equatorial Densities

We first compare the equatorial electron densities as functions of L shell (see Figure 1). The three original diffusive equilibrium models, DE-1, DE-2, and DE-B, perform rather poorly in the near-Earth region. They may

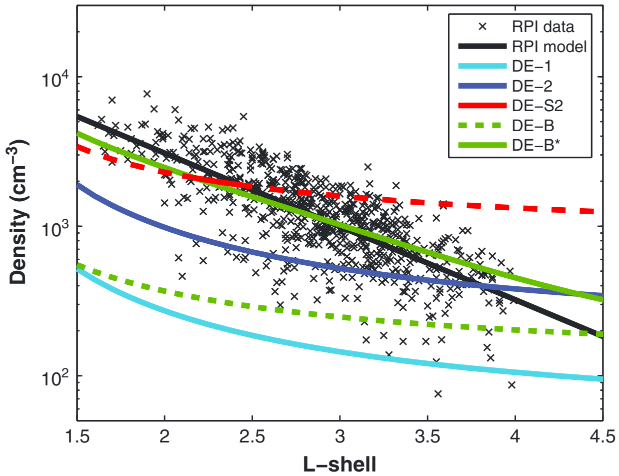

Figure 1. Equatorial electron densities derived from the RPI measurements plotted as a function of L shell are denoted by black crosses. The solid black line is the least squares fit to the data. Solid cyan, blue, and green lines denote the DE-1, DE-2, and DE-B* models, respectively. Red line, representing the DE-S2 model, is solid in the vicinity of $L = 2.3$ and dashed everywhere else. The dashed green line represents the DE-B model.

be off by a factor of up to 10 compared with observation. These large deficiencies can be understood: as we explained in the previous section, the key parameter N_B was determined so as to be consistent with a local observation, but it cannot describe the global density distribution. The DE-S2 and the modified DE-B* models have substantially improved near-Earth predictions. The former used an N_B value better representing the near-Earth density, bringing the DE-S2 model prediction very close to the measured data in the vicinity of $L = 2.3$ (solid portion of the red line), which is where the authors have applied this particular model. However, this did not improve the falloff of the equatorial densities with L value, indicating that the deficiency exists intrinsically in the diffusive equilibrium approximation. Only DE-B* reasonably reflects the L dependence. However, this was achieved by the introduction of an additional six-parameter L shell and radial distance dependence. These parameters were selected in such a way that the resulting equatorial densities match the empirical plasmasphere model of *Carpenter and Anderson* [1992] as close as possible. Such approach has essentially changed the characteristics of the model from the original diffusive equilibrium model to an almost purely empirical model.

Quantitatively, if we describe the density L dependence as a power law, the equatorial densities obtained from RPI measurements are proportional to $L^{-3.07}$. In contrast, the diffusive equilibrium modeled densities decrease as $L^{-0.61}$ to $L^{-1.05}$, which is clearly not steep enough to satisfactorily describe the density distribution. The disagreement between the equatorial profiles of diffusive equilibrium models and measurements is not a new discovery and has been known for several decades (a comprehensive discussion can be found in chapter 5 of *Lemaire and Gringauz* [1998]). As we discussed in section 1, this deficiency in modeling the equatorial densities by itself does not necessarily completely invalidate the diffusive equilibrium approach, since in theory the parameters at the base level may vary significantly with latitude and may fit any given equatorial density profile, such as observed ones, as pointed out by *Carpenter and Smith* [1964]. Note that each equatorial density is mapped along different field lines to the base altitude at different latitudes. Nonetheless, the outcome clearly shows that any use of diffusive equilibrium models (with the additional assumptions of constant temperatures and absence of the centrifugal force) to describe the plasmasphere globally does not produce a representative equatorial density profile. A detailed comparison of several existing empirical models, such as *Carpenter and Anderson* [1992], *Gallagher et al.* [2000], *Sheeley et al.* [2001], and *Denton et al.* [2006], can be found in a paper by *Ozhogin et al.* [2012]. All these empirical models have different slopes of the equatorial L dependence; however, all of them are steeper than any of the diffusive equilibrium models and on average better representing the measured equatorial densities.

In principle, the equatorial L dependence can be derived by choosing different latitudinal and geocentric distance dependence of the base density in diffusive equilibrium models, as done by *Bortnik et al.* [2011]. Nevertheless, none of the diffusive equilibrium models produce the equatorial density distribution that decreases with increasing distance fast enough to represent the RPI-measured densities, indicating that the DE models do not well describe the L dependence of the equatorial density.

3.2. Off-Equator Density Distributions for a Given Radial Distance

To further test whether the diffusive equilibrium approach is valid or not, we examine the behavior of off-equatorial densities for given radial distances. With six varying parameters the diffusive equilibrium models

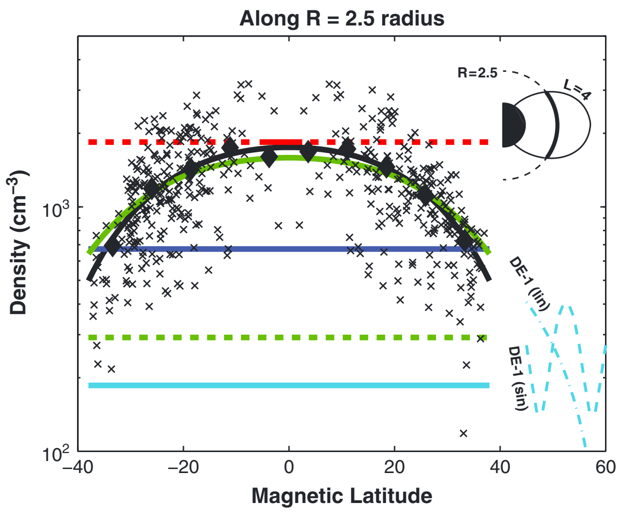

Figure 2. Electron densities along the $R = 2.5\ R_E$ radius derived from the RPI measurements are plotted as a function of magnetic latitude (black crosses). The black diamonds indicate the binned averages of electron densities. The solid black line is the RPI empirical model described by equation (5). Solid cyan, blue, and green lines denote the DE-1, DE-2, and DE-B* models, respectively. The dashed green line represents the DE-B model. Similar to Figure 1, red line, indicating the DE-S2 model, is solid in the vicinity of the region modeled by the authors [*Sonwalkar et al.*, 2011] and dashed everywhere else. The thin cyan dashed and dash-dotted lines are the DE-1 models with the sinusoidal and linear dependences, used to model the subprotonospheric whistlers by *Kimura* [1966]. The thick solid line in the insert in the upper right corner indicates the locations of measured and modeled electron densities.

are very flexible although the chosen parameters may or may not be physical, e.g., the temperatures may be unrealistically high or electron densities at the base level unreasonably low in some latitudes in order to match an observation at altitudes far away from the base. Nonetheless, after applying the assumptions of the isothermal plasmasphere and the absence of centrifugal force, the plasma densities become dependent exclusively on geocentric distance (R) in DE models. Figure 2 compares the observations with several sets of the published DE models at $R = 2.5\ R_E$. The RPI electron density measurements shown in the plot are from a range within $L = 4$ shell (i.e., between −38° and +38° magnetic latitude).

The densities from all four diffusive equilibrium models are constant for a given geocentric distance, while the measured electron densities decrease away from the magnetic equator. As indicated by the binned averages, the densities at ±35° are below 700 (cm^{-3}), and the densities around the equator are above 1700 (cm^{-3}), which is a factor of 2.5 difference. The empirical model derived from the RPI measurements captures this trend. The DE-B* model does as well, although it somewhat overestimates the density at high latitudes and underestimates at low latitudes. In addition to a case of constant electron density at the base of the plasmasphere, section 5 of *Kimura* [1966] describes two modifications of the DE-1 model. The versions of DE-1 model that included linear (thin cyan dash-dotted line) and sinusoidal (thin cyan dashed line) variations with latitude are plotted at magnetic latitudes greater than 45°, which is the region of application of these modifications of the DE-1 model by the author. These versions of DE-1 were used by *Kimura* [1966] for ray tracing between 45 and 60° magnetic latitude to study the subprotonospheric whistlers. It can be clearly seen that the sinusoidal variation can be suitable only for studying local phenomena but not for the description of the whole plasmasphere. The linear variation does produce increased electron density with decreasing latitude, but a linear increase is not realistic. Additionally, if mirrored at the equator, this model would produce a kink in density that has not been seen in observations. When comparing the results within the plasmasphere, we set N_θ constant, same as *Kimura* [1966] did everywhere except section 5. In summary, without significant modifications to the underlying equations and addition of variables, the diffusive equilibrium models are unable to produce realistic off-equator density distributions at a given radial distance.

3.3. Two-Dimensional Distribution and Case Study

The discussion given in section 3.2 shows the difference between the DE models and the RPI measurements on different field lines at locations with the same geocentric distance or, equivalently, constant gravity, further indicating the deficiency of the DE models. One may still argue that there is the possibility of choosing different parameters at the base of different field lines so that the DE models can represent the observations. To remove the ambiguity in the evaluation of the DE models, one has to compare the density along multiple magnetic field lines at the same time. This was impossible before the RPI era. Owing to the unique ability of RPI to make almost instantaneous density measurements along a magnetic field line as the satellite crosses field lines on its orbital plane, we are able to obtain two-dimensional snapshots of the plasmasphere by assuming that the

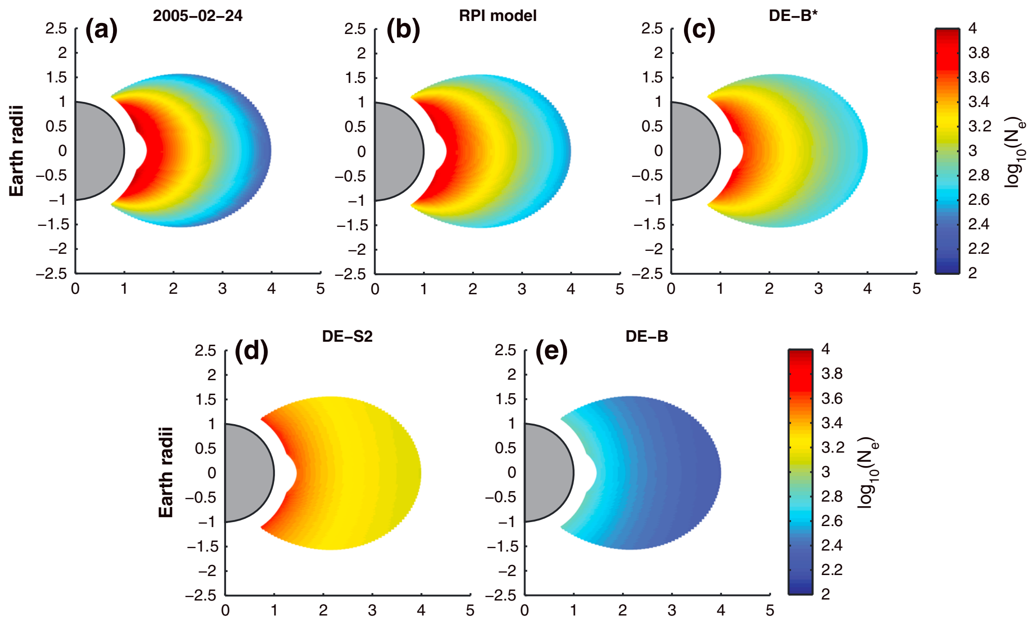

Figure 3. (a) Two-dimensional electron density distribution derived from six electron density profiles obtained from the RPI instrument on 24 February 2005, around 3 MLT. (b) RPI empirical model of the electron density, (c) DE-B* model, (d) DE-S2 diffusive equilibrium model, and (e) DE-B diffusive equilibrium model. All plots are extended from 2000 km altitude and between $L = 1.5$ and $L = 4$.

plasma conditions do not change drastically in the time scale of the plasmaspheric fly through so that successively measured density profiles can be used to construct a 2-D snapshot of the plasmasphere sampled within the segment of the IMAGE orbit.

On 24 February 2005, the RPI produced 6 plasmagrams with clear, sharp, and invertible traces. These measurements were taken within 24 min from 0128 UT until 0152 UT. During this inbound pass, the satellite has moved from $L = 2.92$ to $L = 2.25$, and the corresponding magnetic local times are between 0270 and 0304 MLT. Since this was a geomagnetically quiet period ($Kp = 0$), we can assume that the densities did not change drastically within the time frame of the measurements. First, the equatorial densities from each of the profiles give us the L shell dependence of N_{eq}. Second, by applying a multivariant least squares fit method to all six electron density profiles for the pass, we determine the corresponding fitting parameters: the power index of the cosine function and the multiplier of the magnetic latitude. Relative errors and relative differences between the measured and modeled density profiles are less than 8%. The resulting empirical model for electron density distribution on 24 February 2005 is presented in Figure 3a and is expressed by the following equation:

$$
\begin{aligned}
N(L,\lambda) &= \mathrm{Neq}(L)\cdot \; \cos^{-0.74}\left(\frac{\pi}{2}\cdot\frac{0.99\lambda}{\lambda_{\mathrm{INV}}}\right), \\
\mathrm{Neq}(L) &= 10^{(4.7045-0.5956\cdot L)}
\end{aligned}
\quad (6)
$$

Figures 3b–3e display the outcomes of the models, namely, the RPI model (represented by equation (5)) and the DE-B*, DE-S2, and DE-B models. We only plot two out of four diffusive equilibrium models (DE-S2 and DE-B), since all four have very similar general features. It can be seen that the diffusive equilibrium models produce density distributions that are quite different from the observation, both in the equatorial region and the higher-latitude sectors. Their contour lines are geocentrically circular. Even if the modeled near-Earth equatorial densities are close to the measured ones (i.e., model DE-S2), the slow falloff with distance away from the equator results in very flat density distributions. Correspondingly, if the modeled densities at $L = 4$ were comparable in magnitude to the ones derived from the RPI measurements (i.e., model DE-B), this would result in unrealistically low equatorial densities close to Earth.

Additionally, since the diffusive equilibrium models only depend on geocentric distance, they are unable to reproduce the density decrease with latitude, which is seen in the data. Both DE-S2 and DE-B have differences

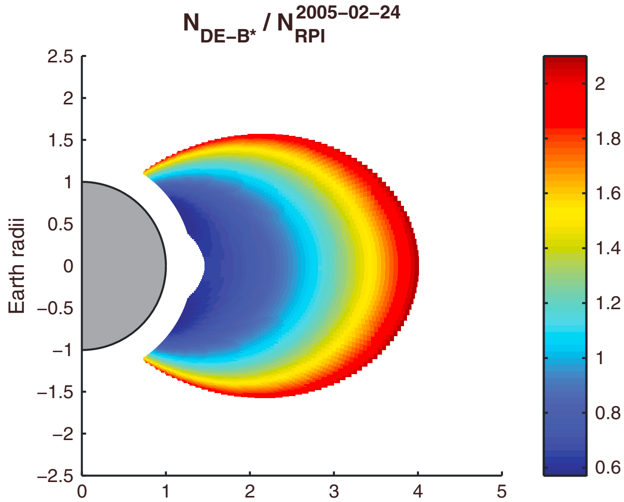

Figure 4. The ratio of the electron densities provided by the model DE-B* and the electron densities measured on 24 February 2005, which are represented by using equation (6).

up to an order of magnitude along the outer edge of the plasmasphere, compared to the densities derived from the RPI measurements. Figure 3 provides a good opportunity to examining the differences/similarities of the models from/to the data and allows us to more fully utilize the potential of measurements from the RPI instrument although the density distribution representation involves approximation and interpolation/extrapolation. The more density profiles we have to construct such images, the better and more accurate are the 2-D snapshots.

The empirical RPI model is very similar to the density distribution derived from the measurements on 24 February 2005, although its radial gradient is slightly smaller. This is understandable as the empirical RPI model is representative of the averaged state of the plasmasphere sampled by the RPI, and at a particular time the distribution can be different. Finally, the modified model DE-B* produces a result that is remarkably close to the measured data. The equatorial density gradient is similar to, although slightly smaller than, the measurements, which may be due to the fact that the DE-B* 12 parameters were chosen in such a way that they match the empirical equatorial density model of *Carpenter and Anderson* [1992], which is consistent with the RPI measurements within the statistical uncertainties . It is somewhat surprising that the latitudinal dependence of the DE-B* model density is, in general, consistent with the observed one. This shows that with a correctly chosen set of 12 parameters, it is possible to create a plasmaspheric density distribution that is reasonably representative of the actual state of the plasmasphere.

While the density distributions along the field lines between DE-B* and observation are similar, there are significant differences both with the radial distance and the latitude, as can be seen from Figure 4. In this particular case, the model DE-B* overestimates densities at $L > 3.5$ by about 100% and underestimates densities at $L < 2$ by about 40%, in other words, roughly agreeing within a factor of 2. This corresponds to underestimation at low latitudes and overestimation at high latitudes of the base densities.

We further investigate the inherent compatibility between the functional form of the DE model/ assumptions. Here we recall that the DE model can be used to fit any given equatorial density profile, as noted by *Carpenter and Anderson* [1992], if the base values are free and that for any given field-aligned density profile, one can fit it to the DE model by varying the temperature or scale height. To test the inherent compatibility between the two, one has to fix the equatorial density for a few field-aligned profiles. To be fair to the DE model we use the DE-B* model that gives six additional free parameters to maximize the flexibility of the model. To remove the factor of fitting parameters we normalize the parameters of the DE-B* model in such a way that the output electron densities from the model match the slope of the equatorial density profile and, at the same time, the field-aligned density profile at a given L shell. By using the least squares fit method, we are able to match the equatorial falloff that is represented by the second equation of (6). Since the diffusive equilibrium densities are a square root of a sum of exponents (equation (3)) and the empirical equatorial densities are described as an exponential falloff with L shell, i.e., due to the different functional forms used, the match is not perfect. However, the differences in the equatorial plane are well within 10%. Simultaneously, we have achieved an almost perfect match (within 1.3%) between the modeled and observed field-aligned electron density profiles at $L = 1.5$. The input parameters that produce such results are $T_{DE} = 1100°K$, $d_d = 2.85$, $L_d = 1.65$, and $W_d = 1.7$ (see the paper by *Bortnik et al.* [2011] for the values of the remaining unchanged parameters). As can be seen from Figure 5, even after such adjustments, there is a ~40% difference at higher-latitude regions, if we ignore the density "bump" around $L = 2.5$ that is due to the imperfect fit of the equatorial profile.

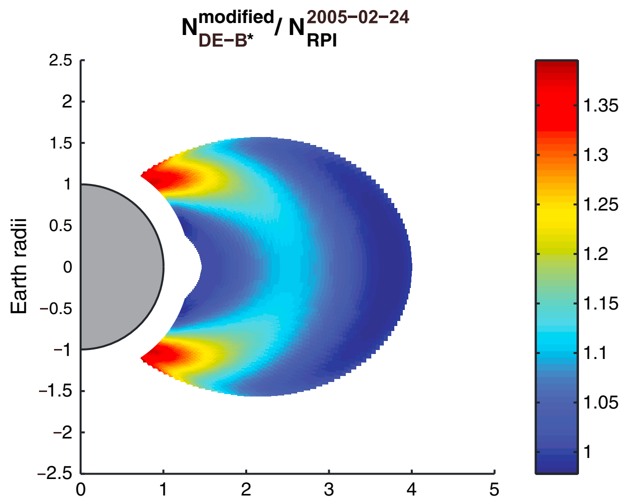

Figure 5. The ratio of the electron densities provided by the modified "best fit" version of the model DE-B* to the electron densities measured on 24 February 2005, which are represented by using equation (6).

3.4. Quantitative Evaluation

After comparing the model results to the measurements in three previous sections, we now statistically analyze the differences between each model prediction and the RPI plasmaspheric measurements. There are multiple ways to perform such a quantitative analysis. In this study we choose the "relative difference" as the measure of how well the model results compared to the experimental measurements. Relative difference is defined as the absolute difference between the model and data values divided by their arithmetic mean, i.e., RD = |Data − Model|/|½Data + ½Model|. Note that the relative difference differs from the relative error, RE = | Data − Model |/Data, which is sensitive and amplifies the difference when a *Data* value is small.

As RD is equal or less than 2, we divide all the results into four categories based on how well the model agrees with the data: "good" for RD = 0 ~ 0.25, "acceptable" for RD = 0.25 ~ 0.5, "poor" for RD = 0.5 ~ 1.0, and "not acceptable" for RD > 1. Within the "good agreement" category the relative difference is practically indistinguishable from the relative error. Within the "acceptable agreement" category (values 0.25–0.50), the difference between them is within 0.1. Thus, if the model and data are reasonably close, both relative error and relative difference are less than 0.50; however, the two approaches become different after this value. Relative errors between 0.50 and 1.00 can mean that the model is either very strongly underestimating or that it is overestimating by a factor of ~2. In contrast, the relative difference between 0.50 and 1.00 means that the model is either higher or lower than the data by about a factor of 3, which we categorize as "poor agreement." Any value that is greater than 1 means that the agreement between model and data is not acceptable. We calculate the relative differences of all four diffusive equilibrium models, as well as the DE-B* model and the RPI empirical model for all 700 profiles in the database. The number of data points that form a given profile ranges from several tens to several hundreds and depends on the sounding program used at the time of the measurement and the length of the echo trace. The total number of data points used is more than 85,000.

Figure 6 plots the values of relative differences for all the models as histograms, where the vertical axis is normalized to the total number of data points and multiplied by 100 to represent the percentage of the model values with a certain relative difference. It can be seen that the results are very diverse. The DE-1 and DE-B diffusive equilibrium models have relative differences greater than 1 (not acceptable according to our definition) for more than 77% of the cases. Such performance is not surprising by looking at the equatorial densities, Figure 1. Since both DE-1 and DE-B exhibit lowest values on the equator, we cannot expect these models to agree with the full density profiles. DE-2 and DE-S2 produce better results: ~25% of the cases in good agreement with data and ~30% in acceptable agreement. However, the DE-B* model performs much better than any diffusive equilibrium models. With 43% of cases in good agreement and 33% in acceptable agreement, it is just slightly below the empirical RPI model.

It is worth noting that the DE-1 model was validated by three topside electron density profiles from Alouette satellite obtained on 9 July 1963 (see Figure 10 of *Kimura* [1966]). These measurements range from 300 km to 1000 km altitude, and they agree with the DE-1 model almost perfectly, meaning that this set of input parameters may be suitable to describe the topside ionosphere up to 1000 km altitude. Similarly, the DE-S1 and DE-S2 models are in good agreement with bottomside ionosonde measurements and DMSP satellite measurements taken on 22 and 26 October 2005, correspondingly, and the IRI-2007 model below 2000 km (see Figure 14 of *Sonwalkar et al.* [2011]). Since these two models were used to derive the densities along a single magnetic field line by the inversion of the whistler mode traces, the correctly chosen set of input

 10.1002/2014JA019982

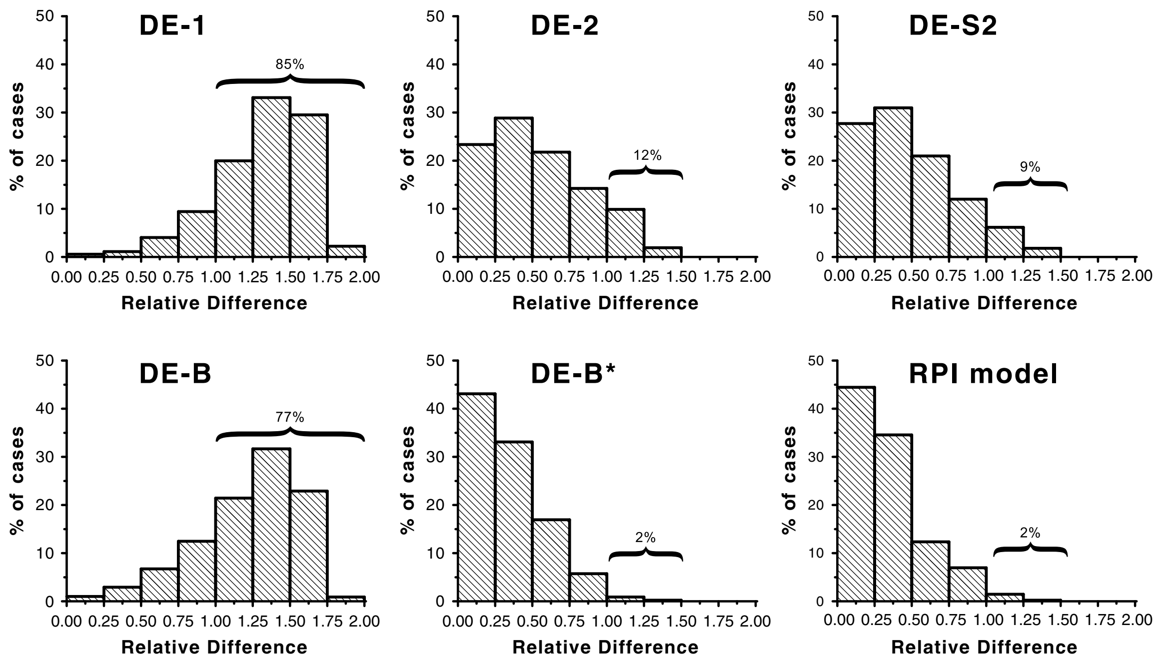

Figure 6. Histograms of relative difference between the RPI-measured electron density profiles and the models.

parameters might adequately describe the density distribution along the given field line. Unfortunately, the RPI instrument was operating in very low frequency mode (below 70 kHz) when the satellite was close to Earth within the plasmasphere, making it impossible to compare the results from inversion of the field-aligned traces and the inversion of whistler traces for the observations on 22 and 26 October 2005.

4. Discussion and Conclusions

We have evaluated four diffusive equilibrium models by comparing them both qualitatively and quantitatively to the 700 plasmaspheric electron density profiles containing over 85,000 individual measurements obtained by the RPI instrument onboard the IMAGE satellite. It is clear from the analysis of the equatorial and off-equatorial profiles, as well as 2-D snapshots of the plasmasphere, that the diffusive equilibrium models are not able to model an electron distribution that is representative of the real plasmasphere. Even if the close-to-Earth densities are in good agreement with the data (i.e., DE-S2), the electron densities at greater distances are in poor agreement due to a smaller equatorial gradient. Similar situations are also with the latitudinal distribution at a given radial distance: if the equatorial densities agree with the data, then higher-latitude values do not. This might be due to several assumptions that are needed in order for the diffusive equilibrium model to work. In particular, the assumption of the constant electron and ion temperatures can be a significant factor. Similarly, the limitation of the force balance along a single field line and the absence of the drift and cross-field motions (i.e., azimuthal and radial) of the particles can be crucial. Yet without such assumptions the analytical form of the equation, which is required by many practical applications, would be difficult or even impossible to derive.

The difficulty for a fair evaluation of the DE models arises from the fact that the DE models often involve many free parameters which smears the boundary between a theoretical model and empirical models. Fundamentally, the DE model, as a theoretical model, was based on the hydroequilibrium as a function of altitude along a field line with the internal electric field coupling the ions and electrons. With this assumption, the original model [*Angerami and Thomas*, 1964] in effect eliminated the pressure gradient forces while retaining the ion gravity force in determining the electric field that couples the two components of the plasma (see their equation (10)). It is now well known that the gravity is not important to maintain the steady state electric field in a collisionless or weakly collisional plasma while the electron pressure gradient force is a dominant term [e.g., *Cravens*, 1997; *Schunk and Nagy*, 2000]. We note that when the electron and ion pressures are different, especially if there are heating mechanisms that heat the electrons and ions at different rates, as indicated by their equation (9), or when the system is not in hydroequilibrium, their equation (10) cannot recover the electric field determined from the generalized Ohm's law. In effect, the model did not describe the coupling between the ion and electron fluids properly. We think that even in steady state the convective terms may play crucial roles in determining the plasma distribution. In contrast, if a system is maintained by the gravity, the reaction (the acceleration by the gravitational force) for electrons and ions is the same. Therefore, the theoretical foundation of the DE models is questionable as a static model.

Nonetheless, the performance of a model can always be improved by introducing more adjustable parameters even if the basic functional form is flawed. The diffusive equilibrium models can create a field-aligned profile to reasonably represent an individual field-aligned density distribution measurement with six varying parameters although these parameters may or may not be physically reasonable as one may see in Table 1, in which the same heavy ion population can range from less than 3% to 90% in different fits. However, the same set of parameters will not adequately describe the whole plasmasphere. It is, in theory, possible to describe a measured distribution, such as in Figure 3a, with a series of DE model fits which multiply the number of fitting parameters, although this is not practical. Here we should emphasize that an empirical model is more useful if it contains few parameters and can describe the dependence of the quantity under a wide range of possible physical conditions.

In conclusion, if the model users need an appropriate representation of the whole plasmasphere, several approaches can be suggested. First, the modified model (DE-B*) is in good agreement with the RPI data. The relative differences between this model and the electron densities derived from the RPI are just slightly underperforming compared to the empirical RPI model, which was derived from the data. Additionally, the DE-B* produces the electron density distribution that is overall similar to the real state of the plasmasphere, at least in one of the examples (see Figure 3). However, the caveats of such approach is that doubling of the number of adjustable parameters makes it difficult to choose an appropriate set of parameters and even more difficult to justify such choice in the absence of satellite or rocket measurements. Another drawback is that the physical parameters themselves (ion composition, temperatures, and densities) lose their original physical meaning. This can be seen from Figure 1, where the solid green (DE-B) that shows the original DE model without the modifications is much lower than the dashed green (DE-B*) line. The differences between the models are large not only in a quantitative sense, but the general properties are different as well.

Second, one can introduce the functional form that would change the temperature or density at the base of the diffusive equilibrium model with latitude, magnetic local time, and/or any other physical factors similar to *Kimura* [1966]. In principle, if correctly defined, such dependence would be able to modify the densities at the base of the diffusive equilibrium model in such a way that the equatorial profile and latitudinal variations would represent the experimentally measured data. While such approach would demand more parameters, which is not always desirable, the original terms of the diffusive equilibrium model will not lose their physical meaning. Finally, another approach is to use the previously developed empirical models for the ray tracing applications. The empirical models are available in the form of a computer code [e.g., *Gallagher et al*., 2000] or an analytical equation [e.g., *Denton et al*., 2006; *Ozhogin et al*., 2012]. The interested readers may refer to *Ozhogin et al*. [2012] for more information about the performance of various empirical models.

Acknowledgments
This work was supported by the NSF grants ATM-0902965 and AGS-0903777 to the University of Massachusetts Lowell. UML's CORPRAL plasmagram prospecting software and NASA Virtual Wave Observatory were instrumental in selection of plasmagrams for our investigation. Product ID for RPI plasmagram data is http://spase.info/VWO/DisplayData/IMAGE/RPI/IMAGE_RPI_PNG_PGM_PT5M. We thank I. Galkin for his support in the use of these tools, S. Mendonca for help with the figures, and J. Bortnik and V.S. Sonwalkar for valuable discussions.

Michael Liemohn thanks Xiaoxin Zhang and Richard Denton for their assistance in evaluating this paper.

References

Angerami, J. J., and D. L. Carpenter (1966), Whistler studies of the plasmapause in the magnetosphere: 2. Electron density and total tube electron content near the knee in magnetospheric ionization, *J. Geophys. Res.*, *71*, 711–725, doi:10.1029/JZ071i003p00711.

Angerami, J. J., and J. O. Thomas (1964), Studies of planetary atmospheres: 1. The distribution of electrons and ions in the Earth's exosphere, *J. Geophys. Res.*, *69*, 4537–4560, doi:10.1029/JZ069i021p04537.

Bauer, S. J. (1962), On the structure of the topside ionosphere, *J. Atmos. Sci.*, *19*, 276.

Benson, R. F., P. A. Webb, J. L. Green, L. Garcia, and B. W. Reinisch (2004), Magnetospheric electron densities inferred from upper-hybrid band emissions, *Geophys. Res. Lett.*, *31*, L20803, doi:10.1029/2004GL020847.

Bortnik, J., L. Chen, W. Li, R. M. Thorne, and R. B. Horne (2011), Modeling the evolution of chorus waves into plasmaspheric hiss, *J. Geophys. Res.*, *116*, A08221, doi:10.1029/2011JA016499.

Burch, J. L. (2000), IMAGE mission overview, *Space Sci. Rev.*, *91*(1–2), 1–14.

Carpenter, D. L., and R. R. Anderson (1992), An ISEE/whistler model of equatorial electron density in the magnetosphere, *J. Geophys. Res.*, *97*, 1097–1108, doi:10.1029/91JA01548.

Carpenter, D. L., and J. Lemaire (2004), The plasmasphere boundary layer, *Ann. Geophys.*, *22*, 4291–4298, doi:10.5194/angeo-22-4291-2004.

Carpenter, D. L., and R. L. Smith (1964), Whistler measurements of electron density in the magnetosphere, *Rev. Geophys.*, *2*, 415–441, doi:10.1029/RG002i003p00415.

Carpenter, D. L., N. Dunckel, and J. F. Walkup (1964), A new very low frequency phenomenon: Whistlers trapped below the protonosphere, *J. Geophys. Res.*, *69*, 5009–5017, doi:10.1029/JZ069i023p05009.

Cravens, T. E. (1997), *Physics of Solar System Plasmas*, Cambridge Univ. Press, New York.

Denton, R. E., K. Takahashi, I. A. Galkin, P. A. Nsumei, X. Huang, B. W. Reinisch, R. R. Anderson, M. K. Sleeper, and W. J. Hughes (2006), Distribution of density along magnetospheric field lines, *J. Geophys. Res.*, *111*, A04213, doi:10.1029/2005JA011414.

Fung, S. F., and J. L. Green (2005), Modeling of field-aligned guided echoes in the plasmasphere, *J. Geophys. Res.*, *110*, A01210, doi:10.1029/2004JA010658.

Gallagher, D. L., P. D. Craven, and R. H. Comfort (2000), Global core plasma model, *J. Geophys. Res.*, *105*, 18,819–18,833, doi:10.1029/1999JA000241.

Helliwell, R. A., J. P. Katsufrakis, and M. L. Trimpi (1973), Whistler-induced amplitude perturbation in VLF propagation, *J. Geophys. Res.*, *78*, 4679–4688, doi:10.1029/JA078i022p04679.

Horwitz, J. L., R. H. Comfort, and C. R. Chappell (1990), A statistical characterization of plasmasphere density structure and boundary locations, *J. Geophys. Res.*, *95*, 7937–7947, doi:10.1029/JA095iA06p07937.

Huang, X., B. W. Reinisch, P. Song, P. Nsumei, J. L. Green, and D. L. Gallagher (2004), Developing an empirical density model of the plasmasphere using IMAGE/RPI observations, *Adv. Space Res.*, *33*, 829–832.

Inan, U. S., and T. F. Bell (1977), The plasmapause as a VLF wave guide, *J. Geophys. Res.*, *82*, 2819–2827, doi:10.1029/JA082i019p02819.

Inan, U. S., T. F. Bell, and R. R. Anderson (1977), Cold plasma diagnostics using satellite measurements of VLF signals from ground transmitters, *J. Geophys. Res.*, *82*, 1167–1176, doi:10.1029/JA082i007p01167.

Kimura, I. (1966), Effects of ions on whistler-mode ray tracing, *Radio Sci.*, *1*, 269–283.

Lemaire, J. F., and K. I. Gringauz (1998), *The Earth's Plasmasphere*, Cambridge Univ. Press, Cambridge, U. K.

Nagai, T., J. Horwitz, R. Anderson, and C. Chappell (1985), Structure of the plasmapause from ISEE 1 low-energy ion and plasma wave observations, *J. Geophys. Res.*, *90*, 6622–6626.

Ozhogin, P., J. Tu, P. Song, and B. W. Reinisch (2012), Field-aligned distribution of the plasmaspheric electron density: An empirical model derived from the IMAGE RPI measurements, *J. Geophys. Res.*, *117*, A06225, doi:10.1029/2011JA017330.

Park, C. G. (1973), Whistler observations of the depletion of the plasmasphere during a magnetospheric substorm, *J. Geophys. Res.*, *78*, 672–683, doi:10.1029/JA078i004p00672.

Reinisch, B. W., X. Huang, P. Song, G. S. Sales, S. F. Fung, J. L. Green, D. L. Gallagher, and V. M. Vasyliunas (2001), Plasma density distribution along the magnetospheric field: RPI observations from IMAGE, *Geophys. Res. Lett.*, *28*, 4521–4524, doi:10.1029/2001GL013684.

Reinisch, B. W., M. B. Moldwin, R. E. Denton, D. L. Gallagher, H. Matsui, V. Pierrard, and J. Tu (2009), Augmented empirical models of plasmaspheric density and electric field using IMAGE and CLUSTER data, *Space Sci. Rev.*, *145*, 231–261, doi:10.1007/s11214-008-9481-6.

Sandel, B. R., J. Goldstein, D. L. Gallagher, and M. Spasojevic (2003), Extreme ultraviolet imager observations of the structure and dynamics of the plasmasphere, *Space Sci. Rev.*, *109*, 25–46.

Schunk, R. W., and A. F. Nagy (2000), *Ionospheres: Physics, Plasma Physics, and Chemistry*, Cambridge Univ. Press, New York.

Sheeley, B. W., M. B. Moldwin, H. K. Rassoul, and R. R. Anderson (2001), An empirical plasmasphere and trough density model: CRRES observations, *J. Geophys. Res.*, *106*, 25,631–25,641, doi:10.1029/2000JA000286.

Song, P., B. W. Reinisch, X. Huang, and J. L. Green (2004), Magnetospheric active wave experiments, in *Frontiers of Magnetospheric Plasma Physics*, COSPAR Colloquia Series, vol. 16, pp. 235–246, Elsevier, London, U. K.

Sonwalkar, V. S., A. Reddy, and D. L. Carpenter (2011), Magnetospherically reflected, specularly reflected, and backscattered whistler mode radio-sounder echoes observed on the IMAGE satellite, Part 2: Sounding of electron density, ion effective mass (meff), ion composition (H^+, He^+, O^+), and density irregularities along the geomagnetic field line, *J. Geophys. Res.*, *116*, A11211, doi:10.1029/2011JA016760.

Starks, M. J., R. A. Quinn, G. P. Ginet, J. M. Albert, G. S. Sales, B. W. Reinisch, and P. Song (2008), Illumination of the plasmasphere by terrestrial very low frequency transmitters: Model validation, *J. Geophys. Res.*, *113*, A09320, doi:10.1029/2008JA013112.

Storey, L. R. O. (1953), An investigation of whistling atmospherics, *Philos. Trans. R. Soc. A*, *246*, 113–141, doi:10.1098/rsta.1953.0011.

Tu, J., P. Song, B. W. Reinisch, and J. L. Green (2007), Smooth electron density transition from plasmasphere to the subauroral region, *J. Geophys. Res.*, *112*, A05227, doi:10.1029/2007JA012298.

Vranjes, J., and M. Y. Tanaka (2005), On gravity induced electric field in space plasmas, *Phys. Scr.*, *71*, 325–328.